Consistency of $^{16}O(n,\alpha)$ cross sections

M. T. Pigni[1,*] and S. Croft[2]
[1]Nuclear Data and Criticality Safety, Oak Ridge National Laboratory, Oak Ridge, Tennessee 37831, USA
[2]Safeguards and Security Technology, Oak Ridge National Laboratory, Oak Ridge, Tennessee 37831, USA

(Received 2 June 2020; accepted 30 June 2020; published 27 July 2020)

The evaluated $^{16}O(n,\alpha)$ cross sections in the ENDF/B-VIII.0 nuclear data library remain uncertain because of systematic discrepancies in the measured data. In the energy region below the first excited state, *R*-matrix analyses rely heavily on the inverse reaction, and in particular, they rely on the measured $^{13}C(\alpha,n)^{16}O$ cross sections reported by Bair *et al.* in 1973 and Harissopulos *et al.* in 2005. The Harissopulos cross section values are systematically lower than those previously reported by Bair. Drawing on the available experimental information, this paper briefly describes and demonstrates that the two sets of measured cross sections are consistent.

DOI: 10.1103/PhysRevC.102.014618

I. INTRODUCTION

Although oxygen is an important element for criticality safety applications in which fissile oxide configurations are present in significant quantities, the related ^{16}O evaluated cross sections in the ENDF/B-VIII.0 library [1] are still uncertain in the (n,α) reaction channel due to systematic discrepancies in the measured data. In the energy region below the first excited state, *R*-matrix analyses [2,3] devoted to generating evaluated cross sections rely heavily on the inverse reaction, and they rely particularly on the measured $^{13}C(\alpha,n)^{16}O$ cross sections reported by Bair *et al.* in 1973 [4] and Harissopulos *et al.* in 2005 [5].

The cross section results of Harissopulos are significantly lower than those of Bair and, being more recent, there is a temptation to favor them in the evaluation. The impact of this would be to scale the $^{16}O(n,\alpha)$ cross sections by a not negligible scaling factor. This has sparked considerable interest and debate, and various arguments to justify such a change have been put forward [6]. In looking at the original reports we are not convinced that the two experiments over the energy range of interest are at odds.

This paper concisely describes and shows that the data sets developed by Bair and Harissopulos are consistent based on the available experimental information. This analysis is fundamentally important for generating the resonance parameters to be included in the next release of the U.S. Evaluated Nuclear Data File (ENDF) library.

II. DISCUSSION

Due to the lack of direct experimental data, the $^{16}O(n,\alpha)$ cross sections are usually obtained by inverse kinematics from measured data on $^{13}C(\alpha,n)^{16}O$ using the reciprocity theorem [7],

$$\sigma_{n\alpha} = \frac{k_\alpha^2}{k_n^2}\frac{g_n}{g_\alpha}\sigma_{\alpha n}, \tag{1}$$

where $g_n, g_\alpha, \sigma_{\alpha n}, \sigma_{n\alpha}, k_\alpha$, and k_n are, respectively, the neutron and α-channel statistical factors, the original (measured) reaction cross section, the inverse reaction cross section, and the α-particle and neutron wave numbers in the center-of-mass frame. Equation (1) can be applied up to the first excited state that in this case is little above 6 MeV. As described in the literature [4,8] and in a note in Bair *et al.* [9], Bair stated that the $^{13}C(\alpha,n)$ thin-target cross sections (shown in purple in Fig. 1) should be reduced by 15–20% to smoothly match his thick-target measurements [8]. The reason for Bair's recommendation can be understood on the basis of a decimal point error found in the figure of thick-target neutron yield published by Macklin and Gibbons [10]. These incorrectly plotted data were most likely used by Bair to normalize the thin-target measured data, but Bair soon realized Macklin's mistake and performed a thick-target measurement [8] to confirm that Macklin's data were plotted as overestimated by an order of magnitude. This would also explain the short sequence of papers submitted and published by Bair. The original plots from Macklin and Bair's thick-target measurements are shown in Fig. 2, whereas digitized and corrected data plotted in Fig. 3 show good agreement between their thick-target measurements above 5 MeV. As an additional check on the normalization factor claimed by Bair, the computation of thick-target yield from Bair's thin-target yield was performed. Namely, the thick-target neutron yield of ^{nat}C can be computed from the thin-target $^{13}C(\alpha,n)$ cross sections $\sigma(E)$ and (e.g., amorphous) mass-stopping power cross sections $L(E)$ as

$$Y_{nat}(E) = \eta\int_0^E \sigma(E')[L(E')]^{-1}dE', \tag{2}$$

where $\eta = N_A\alpha_{nat}/(\alpha_{13}A_{nat})$ is the scaling factor from enriched ^{13}C yield to ^{nat}C yield. The results of the integration

*pignimt@ornl.gov

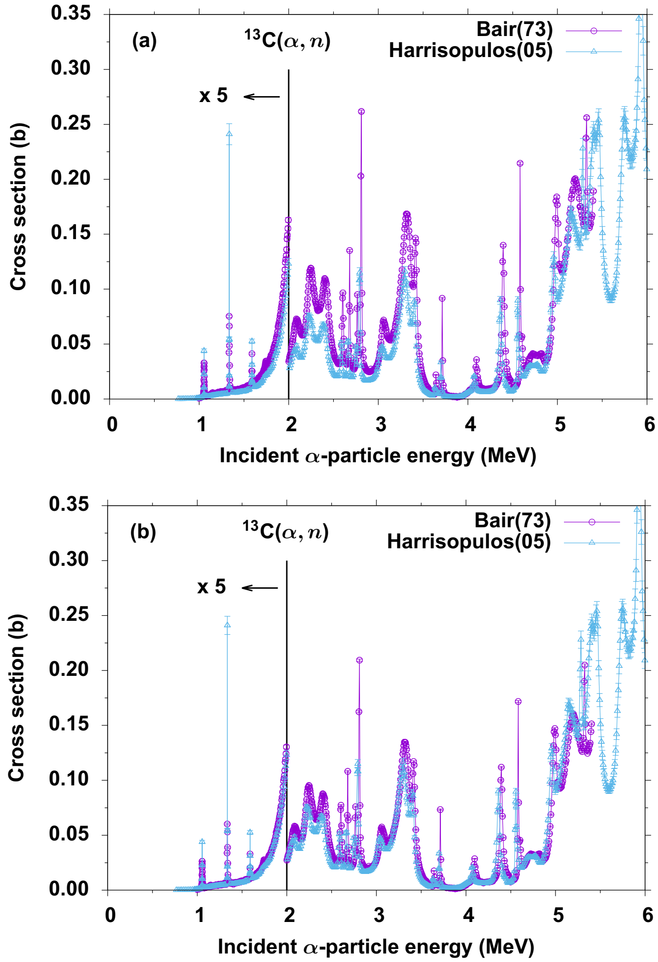

FIG. 1. (a) Plotted ^{13}C(α, n) cross sections and related uncertainties from the EXFOR library entry C0489 for Bair's cross sections in purple and entry F0786 for Harissopulos' data in blue. (b) Plotted ^{13}C(α, n) cross sections from Bair, scaled by −20%. Note linear-linear plots are used for clarity, and below 2 MeV the cross section data are multiplied by 5.

of Eq. (2) shown in Fig. 4 give the same −20% normalization factor predicted by Bair, but most importantly they agree with more recent thick-target measurements performed by West [11]. The same calculations can be performed by using Harrissopulos' thin-target data, resulting in a normalization factor of +15%, as shown in Fig. 5. The thin-target data of Bair and Harissopulos normalized with the calculated factors −20% and +15% are found with an improved agreement up to 5 MeV, as show in Fig. 6. The different energy resolutions of the two experiments might lead to the discrepancy in the resonance peaks, which is mainly visible at ≈1.3 MeV. Above 5 MeV, it is evident that Harissopulos' data are affected by efficiency problems related to the energy dependence of the measured spectrum as the incident α-particle energy E_α is changing. The emission spectrum softens, as evident in the paper by West and Sherwood [11], in which the root-mean-square migration distance is used to correct for the effect which was already modest by design of their detector.

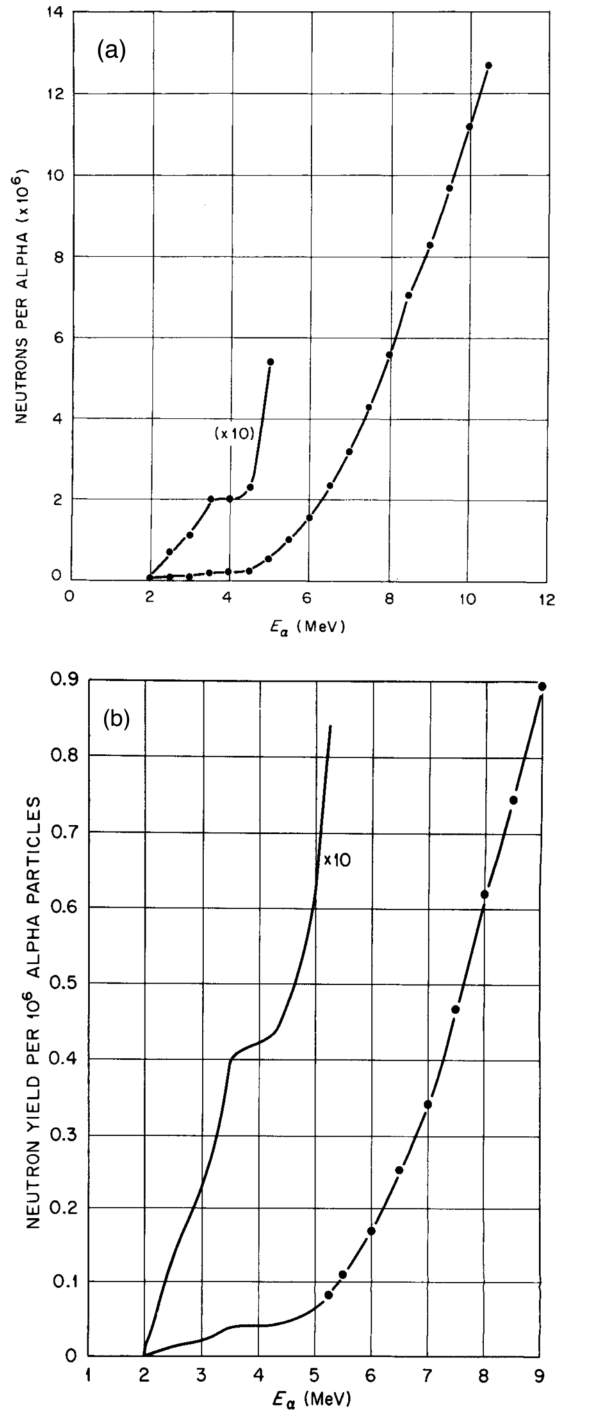

FIG. 2. (a) Data from Macklin [10] showing *a decimal point error*. (b) Data from Bair [8]. The black dots represent measured data, and the solid lines represent thick-target yields calculated from thin-target data. Both figures are copies of the original plots taken from the references above.

Another test of the consistency between two data sets can be performed on the basis of the integral yields. In addition to thin-target data, Bair also quoted a resonance-only integral yield of $Y = 4475 \pm 5\%$ neutron per μC (He$^+$) over the 1.056 MeV resonance for a 100% ^{13}C target. From Bair's measured neutron yield of the narrow resonance at $E_\alpha = 1.054$

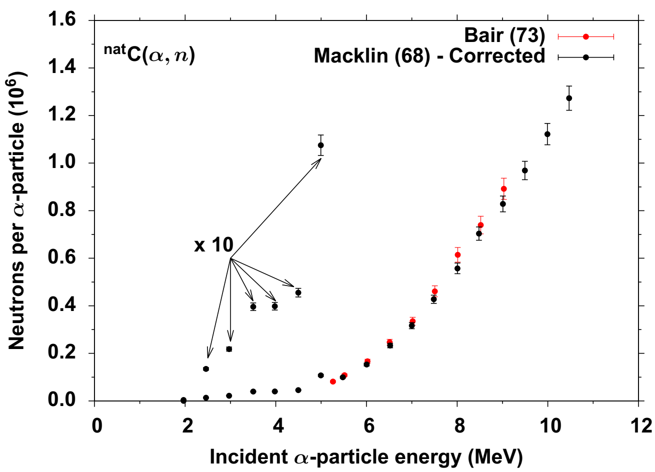

FIG. 3. Total neutron yield vs incident α-particle energy from the digitized data of Bair [8] and Macklin [10]. Macklin's data were corrected by a factor of 10. Below 5 MeV, an additional correction was needed to change from singly charged helium (He$^+$) to doubly charged helium (He^{++}). However, 4.5–5 MeV discrepancies are still visible.

MeV, Harissopulos derived the resonance strength $\omega\gamma = 12 \pm 0.4$ eV, which represents the integral over the resonance width Γ. From the value of the resonance strength [13], one can derive the neutron yield using

$$Y = \omega\gamma \left(\frac{W \frac{N_A}{A}}{2L_\alpha} \right) \frac{\lambda_\alpha^2}{2[E_\alpha/(m_\alpha c^2)]/(1 + m_\alpha/m_{^{13}\mathrm{C}})^3}, \quad (3)$$

where $L_\alpha \equiv L(E_\alpha)$ is the mass stopping power of the incident α particle in the ^{13}C target, $W = 1$ is the weight fraction of the target element, A is the molar mass of the target element,

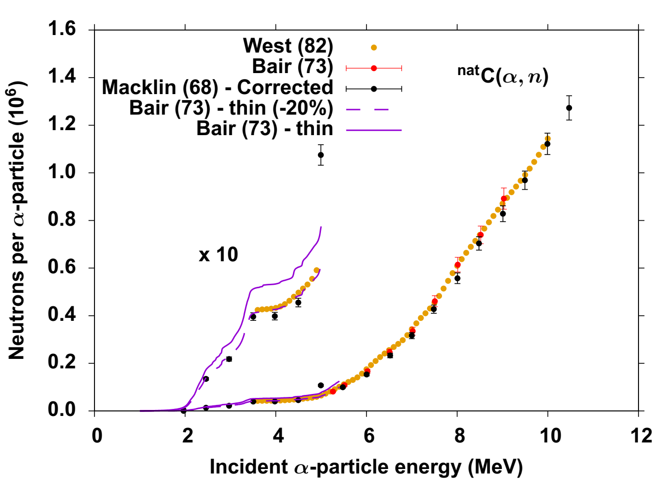

FIG. 4. Total neutron yield vs incident α-particle energy (in purple) calculated from Eq. (2) using Bair's thin-target cross sections. ASTAR [12] mass stopping power cross sections $L(E)$ were used. N_A is the Avogadro number, $\alpha_{13} = 1$ (fraction of ^{13}C in the enriched sample), $\alpha_\mathrm{nat} = 0.0107$ (fraction of ^{13}C in a natural sample), and the $^\mathrm{nat}$C molar mass $A_\mathrm{nat} = 12.010\,735\,9$ g mol^{-1}. The threshold of ^{12}C(α, n) reaction is about 11.4 MeV.

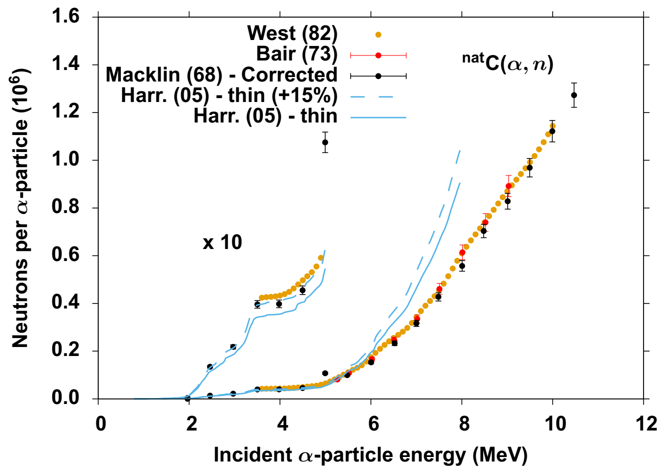

FIG. 5. As in Fig. 4, the neutron yield is computed on the basis of Harissopulos' data (in blue dashed and solid lines). The threshold of ^{13}C(α, n_1) reaction is about 5.05 MeV, and that of ^{13}C(α, n_2) is about 5.12 MeV. As these channels open up, the emission spectrum softens, and the large graphite (Macklin and Bair) and polyethylene (West) moderated assemblies used by these authors are designed to have a flat energy response. In the case of West, corrections were applied.

and N_A is Avogadro's number. The Compton wavelength of the incident α particle is $\lambda_\alpha = hc/(m_\alpha c^2)$. By using the numerical values and constants summarized in Table I, it was found that the neutron yield Y, which is linearly dependent on the resonance strength $\omega\gamma$ measured by Harissopulos, is comparable to the value reported by Bair. Table I reports the values for the neutron yield as calculated by using two values for the mass-stopping power cross sections [12]: one value for graphite, and the other value for amorphous carbon. The yield (graphite) differs from Bair's yield value by -5%, while the yield (amorphous) differs by -10%. The uncertainty of the

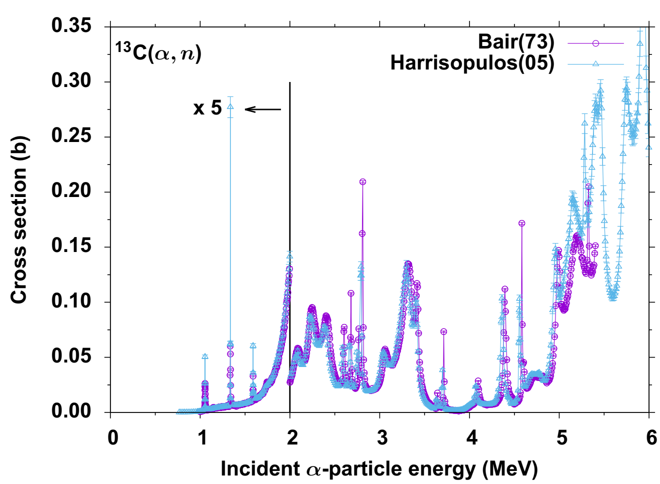

FIG. 6. Plotted ^{13}C(α, n) cross sections and related uncertainties taken from the EXFOR library: entry C0489 for Bair's cross sections in purple, normalized by -20%, and entry F0786 for Harissopulos' data in blue, normalized by $+15\%$ as discussed in the text.

TABLE I. Numerical values and constants used to compute the neutron yield for the resonance at $E_\alpha = 1.054$ MeV on the basis of the resonance strength measured by Harissopulos. The values of the neutron yield are reported for two values of stopping power cross sections: graphite and amorphous carbon [12].

Quantity	Value	Units
E_α	1.054	MeV
m_α	4.002 603 254 15	amu
$m_{^{13}\mathrm{C}}$	13.003 354 837 78	amu
A	13.003 354 837 78	g/mol
$m_\alpha c^2$	3728.401 027	MeV
λ_α	$3.325\,398\,381\,562\,52 \times 10^{-14}$	cm
L_α (graphite)	1863	MeV cm^2/g
L_α (amorphous)	1774	MeV cm^2/g
Y (graphite)	4277.2	n/μC
Y (amorphous)	4072.9	n/μC

Constants used to derive the neutron yield of Eq. (3):
$h = 4.135\,667\,33 \times 10^{-21}$ MeV s
$c = 2.997\,924\,58 \times 10^{10}$ cm/s
amu $= 931.494\,028$ MeV/c^2
$e = 1.602\,176\,487 \times 10^{-19}$ C
$N_\mathrm{A} = 6.022\,141\,791 \times 10^{23}$ mol^{-1}

mass-stopping power values is on the order of 3–5% at about 1 MeV. The combined data from the neutron yield reported by Bair with an uncertainty of 5% and the resonance strength $\omega\gamma$ ($\pm3\%$) reported by Harissopulos lead to the conclusion that the two approaches are in substantial agreement and are certainly not ≈30% apart.

III. CONCLUSIONS

A brief but concise analysis of Bair's and Harrisopulos' available measured data, that are important for the evaluation of the ^{16}O(n,α) cross sections, was performed. The analysis showed that the two measured data sets are consistent when properly normalized to thick-target data. Moreover, this analysis implicitly shows the inconsistency of Harrisopulos' data for incident α-particle energies above about 5 MeV, namely the threshold for the first excited state ^{13}C(α, n_1). This is likely due to an unrecognized sensitivity of the neutron detector used to the emergent spectrum and to a lesser extent the angular distribution.

A new generation of quality (α, n) data is called for in order to reduce reliance on older measurements which were not designed with present demands in mind and did not build in ways to monitor and correct for the changing spectrum with incident energy. The thick-target measurements of West and Sherwood, which we draw on as a consistency check are an exception in this respect but have not been experimentally corroborated nor extended to thin target measurements. The challenges of absolute efficiency determination, current integration, enrichment, purity, and crystallinity of the target, and choice of stopping cross sections limit accuracy but cannot explain the larger discrepancies in the literature. There have been considerable advances in experimental technique and data reporting over the decades and it seems to us timely and necessary to bring these to bear on the problem in a structured way to resurvey the field.

The correct normalization factors derived in this work are of fundamental importance for future R-matrix analyses devoted to generate resonance parameters to be included in the next release of the U.S. ENDF library.

ACKNOWLEDGMENTS

This work was supported by the U.S. Department of Energy (DOE), Nuclear Criticality Safety Program (NCSP) funded and managed by the National Nuclear Security Administration (NNSA) for DOE. ORNL is managed by UT-Battelle, LLC, under Contract No. DE-AC05-00OR22725 for the U.S. Department of Energy. The U.S. government retains and the publisher, by accepting the article for publication, acknowledges that the U.S. government retains a nonexclusive, paid-up, irrevocable, worldwide license to publish or reproduce the published form of this manuscript, or allow others to do so, for U.S. government purposes. DOE will provide public access to these results of federally sponsored research in accordance with the DOE Public Access Plan [14].

[1] D. Brown, M. Chadwick, R. Capote, A. Kahler, A. Trkov, M. Herman, A. Sonzogni, Y. Danon, A. Carlson, M. Dunn, D. Smith, G. Hale, G. Arbanas, R. Arcilla, C. Bates, B. Beck, B. Becker, F. Brown, R. Casperson, J. Conlin, D. Cullen *et al.*, Nucl. Data Sheets **148**, 1 (2018), special issue on Nuclear Reaction Data.
[2] R. O. Sayer, L. C. Leal, N. M. Larson, R. R. Spencer, and Q. R. Wright, Oak Ridge National Laboratory Report No. ORNL/TM- 2000/212, 2000 (unpublished).
[3] L. Leal, E. Ivanov, G. Noguere, A. Plompen, and S. Kopecky, EPJ Nucl. Sci. Technol. **2**, 43 (2016).
[4] J. K. Bair and F. X. Haas, Phys. Rev. C **7**, 1356 (1973).
[5] S. Harissopulos, H. W. Becker, J. W. Hammer, A. Lagoyannis, C. Rolfs, and F. Strieder, Phys. Rev. C **72**, 062801(R) (2005).
[6] M. Chadwick, E. Dupont, E. Bauge, A. Blokhin, O. Bouland, D. Brown, R. Capote, A. Carlson, Y. Danon, C. D. S. Jean, M. Dunn, U. Fischer, R. Forrest, S. Frankle, T. Fukahori, Z. Ge, S. Grimes, G. Hale, M. Herman, A. Ignatyuk *et al.*, Nucl. Data Sheets **118**, 1 (2014).
[7] E. Gadioli, P. E. Hodgson, and E. Gadioli Erba, *Introductory Nuclear Physics* (Oxford University Press, Oxford, 1997).
[8] J. K. Bair, Nucl. Sci. Eng. **51**, 83 (1973).
[9] J. K. Bair and J. Gomez del Campo, Nucl. Sci. Eng. **71**, 18 (1979).
[10] R. L. Macklin and J. H. Gibbons, Nucl. Sci. Eng. **31**, 343 (1968).
[11] D. West and A. C. Sherwood, Ann. Nucl. Energy **9**, 551 (1982).
[12] National Institute of Standards and Technology (NIST), Physical Meas. Laboratory ASTAR database, 2015.
[13] S. Croft and A. Favalli, Nucl. Instrum. Methods Phys. Res., Sect. A **797**, 188 (2015).
[14] http://energy.gov/downloads/doe-public-access-plan.